Int J Clin Exp Pathol 2015;8(2):1247-1258
www.ijcep.com /ISSN:1936-2625/IJCEP0004191

Original Article

M13 phage peptide ZL4 exerts its targeted binding effect on *schistosoma japonicum* via alkaline phosphatase

Yan Liu[1,7*], Shenghui Yang[2*], Jianhua Xiao[1], Liang Yu[1], Li Chen[3], Ju Zou[1], Kegeng Wang[1], Sijie Tan[4], Zhengyang Yu[5], Qingren Zeng[6]

Departments of [1]Parasitology, [4]Histology and Embryology, School of Medicine, [5]Surgical Oncology, First Affiliated Hospital, University of South China, Hengyang, P.R. China; [2]Department of Preventive Medicine and Pathogenic Biology, School of Medicine, Hunan University of Chinese Medicine, Changsha, P.R. China; [3]Department of Medicine, Perelman School of Medicine, University of Pennsylvania, Philadelphia, USA; [6]Centre of Cell and Molecular Biology Experiment, Xiangya School of Medicine, Central South University, Changsha, P.R. China; [7]Hunan Province Cooperative Innovation Center for Molecular Target New Drug Study, Hengyang, P.R. China. [*]Equal contributors.

Received November 27, 2014; Accepted January 28, 2015; Epub February 1, 2015; Published February 15, 2015

Abstract: The present study was to determine the targeting effect of M13 phage peptide ZL4 (MppZL4) on Schistosoma japonicum (S.j). Mice infected with S.j were injected with MppZL4. Real-time PCR was used to detect the distribution and metabolism of MppZL4 in the livers and lungs of mice. In vivo refusion test was performed to detect the targeting of MppZL4. Western blotting was employed to determine the expression of MppZL4. Live imaging was used to detect the distribution of oligopeptide MppZL4. Immunohistochemistry was employed to determine MppZL4 location on adult S.j body surface. Gomori method was employed to detect the influence of oligopeptide MppZL4 on alkaline phosphatase activity. The distribution and metabolism of MppZL4 and M13KE are not significantly different from each other at each time point. The abundance of MppZL4 is changed as S.j migrates in mice. The targeted binding effect of MppZL4 varies at different stages. ZL4 oligopeptide targets S.j in mice. The specific binding sites of MppZL4 on S.j body are mainly located in syncytial cells. The binding sites of MppZL4 on S.j body surface might be ALP or ALP-related proteins. MppZL4 had targeted binding effect on S.j with its binding site being associated with proteins related to S.j alkaline phosphatase. S.j tegument had a specifically binding site with exogenous peptides, offering new means to explore the interactions between hosts and parasites. Additionally, MppZL4 can possibly be used as targeting molecules in worm-resistant drugs or as tracing molecules in imaging diagnosis technologies.

Keywords: *Schitosoma japonicum*, MppZL4, alkaline phosphatase

Introduction

Schistosoma japonicum (*S.j*) are parasitic worms that can result in infections in human bodies, leading to a disease termed schistosomiasis. Schistosomiasis is reported by the World Health Organization as the second most devastating parasitic disease, with hundreds of millions infected in the world. This disease is especially serious in the lake areas of South China [1-7]. The surface membrane of *S.j* has direct contacts with the host and possesses many proteins that are closely related to vital movements of *S.j*. Therefore, in-depth knowledge of the cortex of *S.j*-binding peptide is needed.

In recent years, M13 phage peptide ZL4 (MppZL4) was constructed in live schistosomula using phage differential screening technology [8, 9]. MppZL4 is a molecule composed of M13 phage and ZL4 peptide. MppZL4 can specifically bind to *S.j* at different developmental stages in addition to *S.j* cercaria. Five specific bands can be probed by MppZL4 after transferring *S.j* surface proteins to nitrocellulose membrane, with the largest band being 24 kDa [8], which is close to the molecular weight of *S.j* alkaline phosphatase (ALP; SJCHGC07313; GenBank accession No. AAX26426) [10].

The distribution of ALP at different developmental stages of *S.j* is different. In *S.j* miracidia, the

whole body has strong positive reactions [11]. In *S.j* cercaria, the front part of the worm body shows no enzymatic activity, while the front 1/3 part of tail section has enzymatic activity. In skin schistosomules, ALP is abundant in rear end tissues. When the worms mature, ALP levels in the tegument of the worms are rich [12]. ALP is closely related to the absorption and transportation of glucose. In addition, ALP participates in the transformation from carbohydrates to lipids. ALP is also involved in the metabolism of nucleic acids and proteins, playing an important role during the formation and maintenance of the skin [13, 14]. In this study, we investigated whether MppZL4 had targeted binding effect on *S.j* and its mechanism of action at molecular levels.

Materials and methods

Animals and reagents

All animal care and procedures were conducted according to the guidelines for animal use in toxicology (Society of Toxicology USP, 1989). The field samples of positive Chinese mainland strain snails were kindly provided by Hunan Institute of Schistosomiasis Prevention. Outbreed Kunming strain of mice, 6-8 weeks in age and 35-40 g in weigh, were purchased from Animal Department of Central South University. M13 phage (M13KE for negative control) was purchased from Beverly, MA, USA. MppZL4 phage was amplified after screening in our laboratory. MppZL4 small peptide labeled with Cy5.5 was synthesized by GenScript Inc. (Nanjing, China). Horseradish peroxidase-conjugated monoclonal antibody against M13 (HRP-M13 McAb) were purchased from GE Healthcare Bio-Sciences (Pittsburgh, USA). Mouse monoclonal antibody against M13 (M13 McAb) and mouse monoclonal antibody against β-tubulin (β-tubulin McAb) were purchased from Abcam Inc. (Cambridge, MA, USA).

Real-time polymerase chain reaction (PCR)

A total of 22 male and 22 female mice were randomly divided into 11 groups with 4 mice (2 males and 2 females) in each group. After injection of MppZL4 (1×10^{12} pfu per mouse) through tail vein, livers and lungs were removed directly, without heart lavages at 1 min, 5 min, 10 min, 30 min, 60 min, 1 h, 2 h, 6 h, 12 h, 24 h, 48 h, and 72 h. Then, livers and lungs were cut into pieces and homogenized. After washing with 0.1% Tris buffered saline with Tween 20, the supernatants were discarded. Phages bound to liver and lung tissues were eluted, respectively, and sediments were collected with polyethylene glycol/NaCl to reach a volume to 1 ml. Real-time PCR was employed to determine titers of phages in each group using M13 phage as negative control [15]. Triplicate experiments were carried out in parallel. Sense primer of MppZL4: 5'-TTCGCAATTCCTTTAGTGGT-3'; Anti-sense primer of MppZL4: 3'-TGGGATTTTGCTAAACAACTTTC-5'. Sense primer of M13KE: 5'-GGCGCAACTATCGGTATCAA-3'; Anti-sense primer of M13KE: 3'-CGGCCGAGTGAGAATAGAAA-5'.

The PCR amplification system was composed of 1 μl phage template, 0.6 μl of either sense or anti-sense primer (0.3 μmol/L) and 10 μl of 2 × SYBR Green PCR Master mix, complemented to a total of 20 μl with H_2O. The reaction condition was 95°C for 30 s, followed by 40 circles at 95°C for 30 s, 60°C for 30 s, and 72°C for 1 min.

In vivo refusion test

Eighty mice, including 40 males and 40 females, were randomly divided into 4 experimental subgroups and 4 negative control subgroups with 10 mice in each subgroup after being infected with 200 ± 20 *S.j cercaria*. Another 40 uninfected mice, including 20 males and 20 females, were randomly divided into 4 blank control subgroups with 10 mice in each subgroup. The 4 experimental subgroups were injected with MppZL4 (a dosage of 10^{12} pfu) 3, 10, 24 and 42 days after infection with *S.j cercaria*, respectively. The 4 negative control subgroups were injected with M13KE (a dosage of 10^{12} pfu) 3, 10, 24 and 42 days after infection with *S.j cercaria*, respectively. The 4 blank control subgroups were injected with MppZL4 (a dosage of 10^{12} pfu) without being infected with *S.j cercaria*. Six hours after injection with phages, the mice were sacrificed to collect livers and lungs without heart perfusion being administered. The experiment dates were comprehensively evaluated with both drug targeting index (DTI) and drug selectivity index (DSI) in targeting drug delivery system (TDDS, MppZL4 phage) and conventional drug delivery system (CDDS, M13KE phage) [16-20].

Table 1. Phage titration, DTI and DSI in the lungs and livers of mice (× 10^7 pfu)

Groups	Day 3		Day 10		Day 24		Day 42	
	Lungs	Liver	*Lungs*	Liver	*Lung*	Liver	*Lung*	Liver
Experimental groups	*14.74 ± 0.370*	0.97 ± 0.124	*0.84 ± 0.115*	24.88 ± 0.970	*0.80* ± 0.010	5.02 ± 0.031	*0.88* ± 0.024	20.08 ± 0.792
Negative control groups	*0.90 ± 0.040*	0.95 ± 0.041	*0.85 ± 0.029*	0.90 ± 0.046	*0.84* ± 0.012	0.91 ± 0.016	*0.91* ± 0.014	0.97 ± 0.021
Blank control groups	0.93 ± 0.034	1.02 ± 0.038	*0.79 ± 0.034*	0.95 ± 0.032	*0.90* ± 0.020	0.99 ± 0.019	*1.01* ± 0.017	0.90 ± 0.024
DTI	*16.38*	1.02	*0.99*	27.64	*0.95*	5.52	0.97	20.70
DSI	*15.85*	0.95	*1.06*	26.19	*0.89*	5.07	0.87	22.31

Note: DTI, drug targeting index; DSI, drug selectivity index.

DTI = drug concentration in targeting tissue after t hours of TDDS/drug concentration in targeting tissue after t hours of administration of CDDS;

DSI = drug amount in targeting tissue at t hours/drug amount in non-targeting tissue at t hours.

In the present study:

DTI = the eluted amount of MppZL4 from liver or lung tissues of infected mice at 6 h after MppZL4 injection/the elution amount of M13KE from liver or lung tissues of infected mice at 6 h after M13KE injection;

DSI = the eluted amount of MppZL4 from liver or lung tissues of infected mice at 6 h after MppZL4 injection/the elution amount of MppZL4 from liver or lung tissues of normal mice at 6 h after MppZL4 injection (**Table 1**).

Western blotting

The mice were sacrificed and the livers and lungs were collected without the administering of heart perfusion. Liver tissue (0.1 g per mouse) was fully grinded in a precooled mortar containing a moderate amount of liquid nitrogen. Afterwards, 1000 μl cell lysis buffer containing protease inhibitor was added for homogenization using a glass homogenizer [8]. DNase I (20 μg/ml) and RNase A (5 μg/ml) were then added for a 15-min reaction at 4°C, followed by 5 min of vibration and 45 min of 25,000 g centrifugation at 4°C. Clear supernatant containing soluble protein was carefully collected and quantified using bicinchonininc acid method (Pierce, Rockford, IL, USA) [21]. Lung tissue protein was extracted using identical procedures.

Tissue samples were diluted to 1/4 with loading buffer and denaturized in boiling water for 3 min. Protein (10 μg) underwent electrophoresis using 20 mA for 4 hours at 4°C. Then, the samples were electrotransferred to nitrocellulose membrane (Pall Corporation, USA) at 120 V using a Minigel Transfer Unit (Bio-Rad Laboratories, Hercules, CA, USA) in 4 h. After blocking for 1 h at room temperature using PBS with Tween-20 containing 5% skim milk powder followed by 3 times of washing with Tris buffered saline, the nitrocellulose membrane was kept in horseradish-peroxidase/mouse anti-M13 antibody (1:1000) and 4°C overnight. Enhanced chemiluminescence (Santa Cruz Biotechnology, Texas, USA) was used to visualize the reactions [8, 16]. Each sample was probed with a rabbit anti-β-tubulin antibody (Abcam, Cambridge, MA, USA) as a loading control. The bands were analyzed using Volum Contour of Quantity One Software (Bio-Rad Laboratories, Hercules, CA, USA) [8, 22].

In vivo imaging

Two groups of mice (15 mice per group) on day 3 or day 10 after infection by *S.j* were injected with 100 μl Cy5.5-labeled ZL4 short peptide (Cy5.5-ZL4, 10 μM) via tail vein. Mice injected with Cy5.5-labeled random 12 peptide (Cy5.5-r12P) were used as negative control, and those injected with PBS were used as blank [23]. At 20 min, 6 h, 24 h, 48 h and 72 h after injection [24], fluorescence imaging was performed using IVIS Imaging System 200 Series under 675 nm excitation wavelength and 695 emission wavelength, and images were analyzed using Living Image 3.0 software (Caliper Life Sciences, Alameda, CA, USA). A Cy5.5 filter set was used for acquiring the fluorescence of Cy5.5-MppZL4. Identical illumination settings (lamp voltage, filters, time of exposure, fields of views, binning) were used for acquiring all images. Fluorescence emission images were normalized and reported as photons per second per centimeter squared per steradian (p/s/cm^2/sr). All near-infrared fluorescence images were acquired using 1 s exposure time. During injection and image acquiring process, the mice were anesthetized with 5% chloral hydrate [25].

Immunohistochemistry

Ten mice (5 males and 5 females, and 6-8 weeks) were infected with 200 ± 20 *S.j cercaria* and randomly divided into 2 groups of 5 mice. The mice in both groups were injected with MppZL4 or M13KE phages at a dosage of 1×10^{12} pfu through tail vein 24 days after infection. After 20 min and 6 h, the mice were sacrificed to collect *S.j cercaria*. Afterwards, agar-paraffin double embedding and slicing was performed [26]. Antigen repair was carried out after inactivating the endogenous peroxidase, followed by blocking with working solution containing normal goat serum. After washing 3 times, 100 μl monoclonal antibody anti-M13 (diluted with

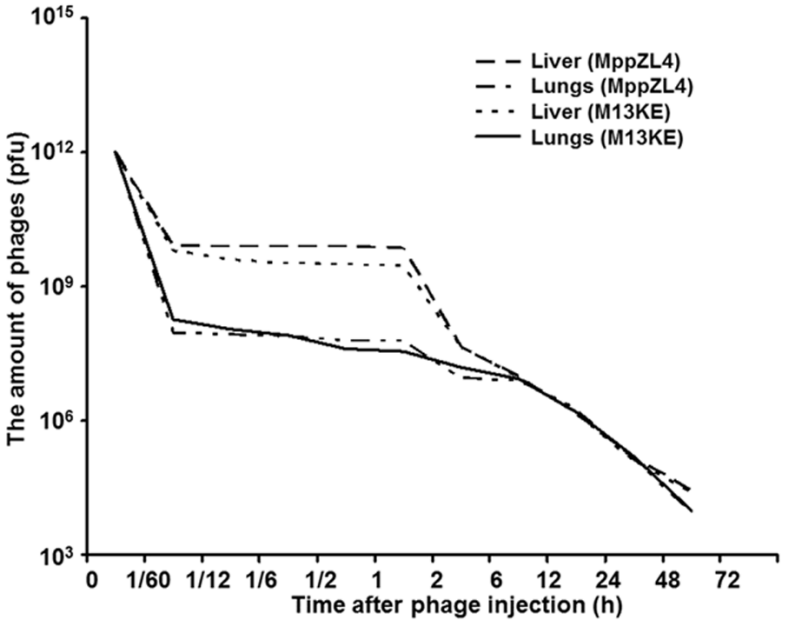

Figure 1. Distribution and metabolism of M13 phages in the liver and lungs of normal mice. The amount of phages in the liver and the lungs at different time points after phage injection were measured and plotted.

Tris-buffered saline to 1:5000) was added and left in 4°C overnight, followed by 6 times of washing with PBS with Tween 20. Horseradish peroxidase-immunoglobulin G was added for a 60-min reaction at 37°C before washing for 6 times, followed by 3,3'-diaminobenzidine staining for 20 min. Mounting was carried out after a normal procedure of hematoxylin staining, dehydration and transparency. Positively stained worms were observed and counted under a microscope [8, 9, 27].

Gomori method

Twelve mice (6 males and 6 females, and 6-8 weeks) were randomly divided into 3 groups of 4 mice. On day 24 after infection with 200 ± 20 *S.j* cercaria, each mouse was injected with 100 μl ZL4 peptide (10 μM, experimental group), random 12 peptides (r12P, control group) or PBS (blank group) through tail vein. After 6 hours, the mice were sacrificed and the worms were collected. Slicing was conducted after agar-paraffin double embedding [22]. The slices were incubated in ALP at 37°C for 2 h. After 2-3 times of washing with distilled water (1 min each time), 2% calcium nitrate was added for 2 min reaction and 2% cobalt nitrate solution was added for another 2 min reaction, followed by 2-3 times of washing as stated above. Then, the slices were reacted with 1% ammonium sulfide for 1 min and washed for several minutes with tap water. Afterwards, drying, dehydration, transparent and gum cementing were sequentially carried out [28]. Finally, microscope observation was performed [29, 30].

Statistical analysis

All data were presented as means ± standard deviations, unless otherwise noted. Data were analyzed using Analysis of Variance, and P values < 0.05 were considered statistically significant. All statistical analyses were performed using SPSS 11.5 software (Chicago, USA).

Results

Distribution and metabolism of MppZL4 and M13KE are not significantly different from each other at each time point

To determine the distribution and metabolism of phages in normal mice, the number of phages was measured. Within the first hour after injection, the liver could bind a large number of phages, which was about 100 times higher than those bound to the lung tissues. At 6 h time point, the numbers of eluted phages were not significantly different between the liver tissues [(0.98 ± 0.037) × 10^7 pfu] and the lung tissues [(0.88 ± 0.062) × 10^7 pfu]. After 6 hours, the concentrations of eluted phages from liver and lung tissues were in the same order of magnitude. The metabolic cycle of phages was about 72 h (**Figure 1**). These data suggested that the metabolism of MppZL4 and M13KE were not significantly different from each other at each time point.

Abundance of MppZL4 is changed as S.j migrates in mice

To detect the target of MppZL4 at different stages of worms, *in vivo* refusion test was performed in different time segments to investigate the distributions of MppZL4 and M13KE in the lungs and liver tissues of mice, as well as targeting and selectivity indexes. DTI and DSI values of eluted phages in lung tissues were 16.38 and 15.85, respectively, on Day 3 in

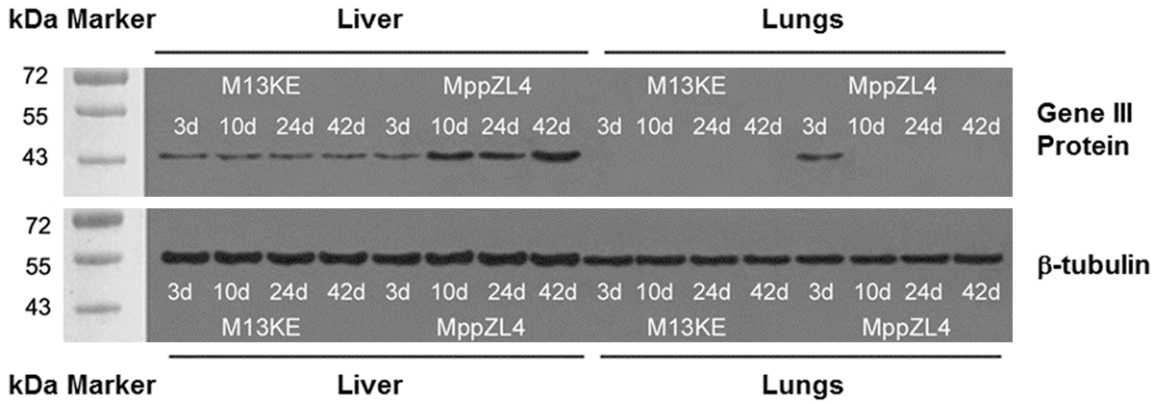

Figure 2. The levels of M13KE and MppZL4 protein expression in the liver and lungs of mice at different time points after infection by *Schistosoma japonicum*. Protein (10 μg) underwent electrophoresis using 20 mA for 4 hours at 4°C. Then, the samples were electrotransferred to nitrocellulose membrane. After blocking for 1 h at room temperature, the nitrocellulose membrane was kept in horseradish-peroxidase/mouse anti-M13 antibody (1:1000) and 4°C overnight. Enhanced chemiluminescence was used to visualize the reactions. Each sample was probed with a rabbit anti-β-tubulin antibody as a loading control.

experimental subgroup, which were much greater than 1. Although the DTI value of eluted phages in the liver was 1.02 (greater than 1), the eluted volume of phages in liver tissues of experimental subgroup had no significant difference compared with those in the negative control and blank control subgroups according to (one-way analysis of variance). By contrast, the eluted phage volume in the lungs of experimental subgroup was much higher than those in the negative control and blank control subgroups. On Day 10, DTI and DSI values of eluted phages in the liver were 27.64 and 26.19, respectively, while DTI and DSI values in the lungs were 0.99 and 1.06, respectively. According to One-Way ANOVA, eluted volume of phages in the liver in the experimental subgroup was much higher than that in the negative control subgroup and the blank control subgroup. By contrast, the eluted volume of phages in the lungs in the experimental subgroup was not significantly different from those in the negative control and blank control subgroups. On Day 24, DTI and DSI values of eluted phages in the liver were 5.52 and 5.07, respectively, while those in the lungs were 0.95 and 0.89, respectively. Eluted volume of phages in the liver in the experimental subgroup was much higher than those in the negative control and blank control subgroups, while eluted volume of phages in the lungs was not significantly different from those in the negative control and blank control subgroups. On Day 42, DTI and DSI values of eluted phages in the liver were increased to 20.70 and 22.31, respectively, while DTI and DSI values of eluted phages in the lungs were 0.97 and 0.87, respectively. Eluted volume of phages in the liver in the experimental subgroup was much higher than those in the negative control and blank control subgroups, while eluted volume of phages in the lungs in the experimental subgroup was not significantly different from those in the negative control and blank control subgroups (**Table 1**). These data suggested that the abundance of MppZL4 was changed as *S.j* migrated in mice.

Targeted binding effect of MppZL4 varies at different stages

To measure the expression of M13KE and MppZL4, Western blotting assay was performed. The results showed that β-tubulin loading control was evident. In addition, specific bands of MppZL4 were observed in mouse liver tissues at different time points after infection, especially on days 10, 24 and 42. There was one specific band of MppZL4 in mouse lung tissues on day 3 after *S.j* infection, without specific bands on days 10, 24, or 42. For M13KE, there was no significant band in lung tissues, but significant bands were observed in liver tissue at all time points (**Figure 2**). The molecular weight is 45.0 kDa, which has the same size with gene III protein of M13 phage. These data suggested that the targeted binding effect of MppZL4 varied at different stages.

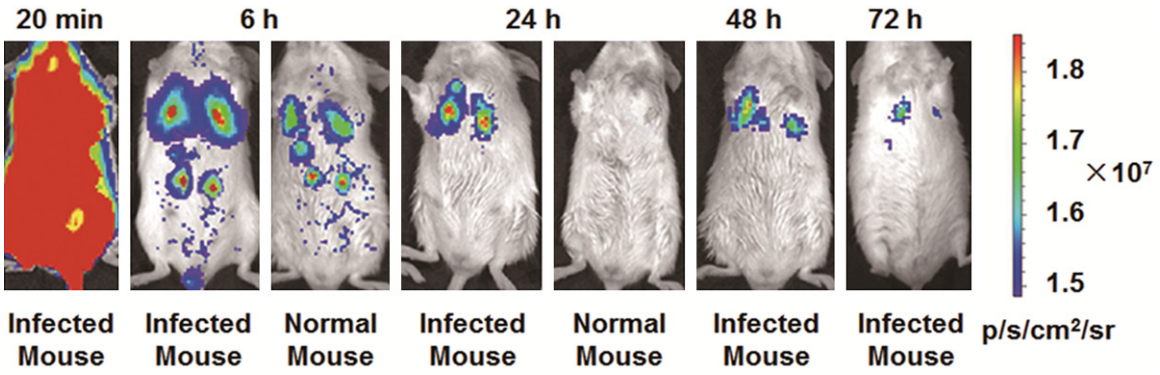

Figure 3. Fluorescence images of mice infected with *Schistosoma japonicum* for 3 days. *In vivo* fluorescence imaging of mice infected with *Schistosoma japonicum* 3 days after intravenous injection of 1.0 nmol Cy5.5-MppZL4. The fluorescence in the lungs can be clearly visualized as indicated from 20 min to 72 h. The fluorescence intensity was recorded as per second per centimeter squared per steradian (p/s/cm^2/sr).

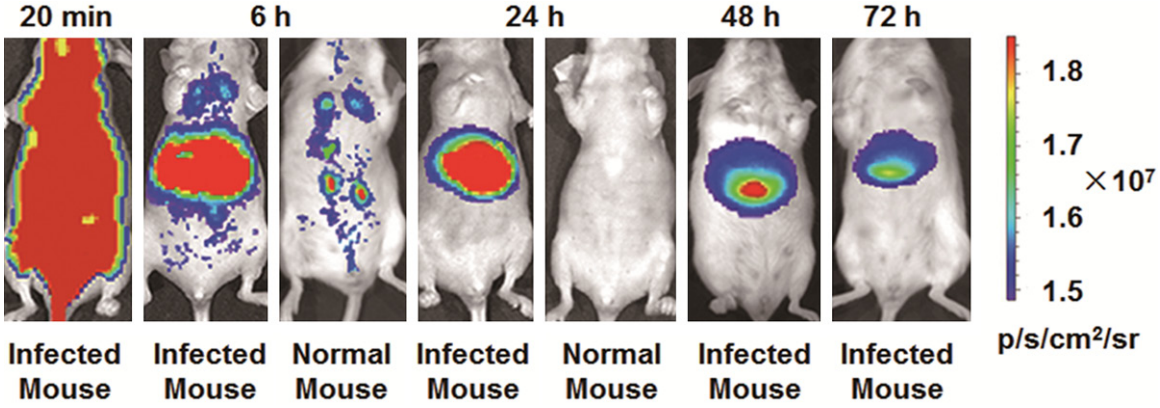

Figure 4. Fluorescence images of mice infected with *Schistosoma japonicum* for 10 days. *In vivo* fluorescence imaging of mice infected with *Schistosoma japonicum* 10 days after intravenous injection of 1.0 nmol Cy5.5-MppZL4. The fluorescence in livers can be clearly visualized as indicated from 20 min to 72 h. The fluorescence intensity was recorded as per second per centimeter squared per steradian (p/s/cm^2/sr).

ZL4 oligopeptide targets S.j in mice

To detect the distribution of oligopeptide MppZL4 in mice bodies, near infrared fluorescence images were taken. For mice being infected by *S.j* for 3 days intravenous injection of 1.0 nmol Cy5.5-ZL4 through tails was performed immediately before experiments. Significant signal accumulation was observed all through mouse bodies from 20 min time point (**Figure 3**). After 6 hours, signals from the lungs of infected mice were significantly stronger than those of healthy mice, with optical signals being observed in the liver and both kidneys. After 24 hours, signals from the liver and both kidneys of infected mouse disappeared, with signals in the lungs being significant, while no significant signals were observed in healthy mice after 24 hours. After 48 hours, signals from the lungs of infected mice were decreased. After 72 hours, there were still significant signals in the right lung, but only decreased signals in the left lung. In addition, only weak signals were observed in the liver after 72 hours (**Figure 3**).

Ten minutes after the intravenous injection of 1.0 nmol Cy5.5-ZL4 through tails, the bodies of mice being infected by *S.j* for 10 days showed significant signal accumulation. After 6 hours, signals from the liver of infected mice were significantly stronger than those from healthy mice, with optical signals being observed in the lungs and both kidneys. After 24 hours, signals in the lungs and both kidneys of infected mice disappeared, with significant signals being visualized in the liver. After 48 hours, signals in

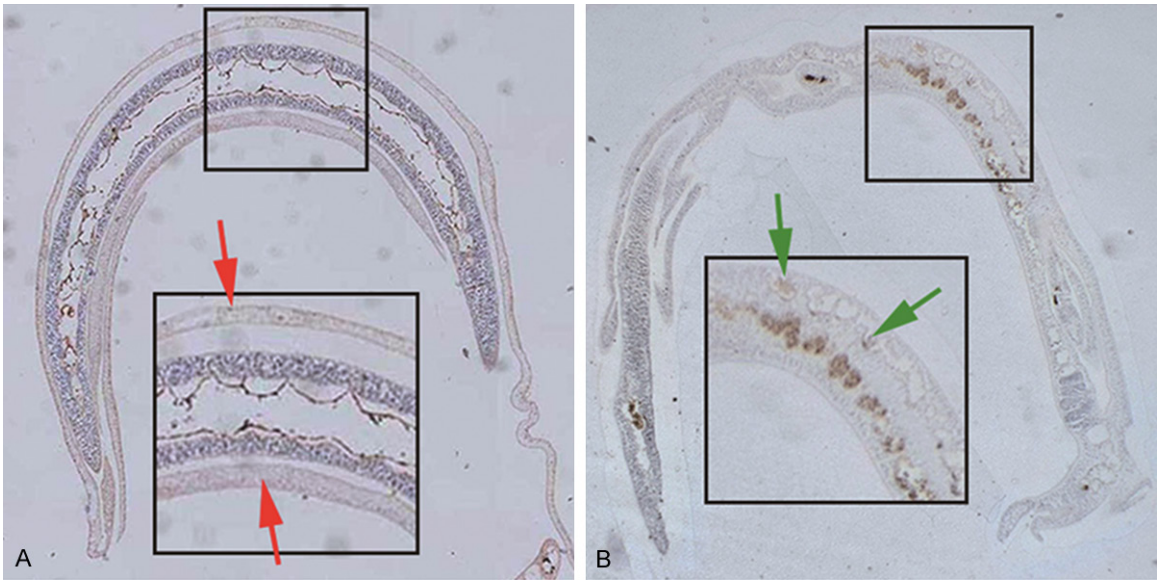

Figure 5. MppZL4 binding to *Schistosoma japonicum* adults. Mice were sacrificed to collect *S.j cercaria*. Afterwards, agar-paraffin double embedding and slicing was performed. Immunohistochemical staining was carried out before positively stained worms were observed and counted under a microscope (× 100). A. Strong reactivity on the tegumental ectoplasts of the worms 20 minutes after injection as indicated by red arrows. B. Positive particles observed in syncytium cells 6 h after injection as indicated by green arrows.

the liver of infected mice were. After 72 hours, significant fluorescence signals were still accumulated in the liver (**Figure 4**). These data indicated that ZL4 short peptide could target *S.j* in mice.

Specific binding sites of MppZL4 on S.j body are mainly located in syncytial cells

To determine the location of MppZL4 on adult *S.j* body surface, the affinity of MppZL4 for the surface of *S.j* was investigated at 20 min and 6 h after injection. Strong reactivity was evident on the tegumental ectoplasts of the worms 20 minutes after injection (**Figure 5A**, red arrows). By contrast, positive particles were observed in syncytium cells 6 h after injection (**Figure 5B**, green arrows). The positive rates were 78% (39/50, 15 min) and 64% (32/50, 6 h), having no significant differences (χ^2 test, $P < 0.05$). Negative results were obtained for worm bodies treated with M13KE phages (data not shown). These data suggested that the specific binding sites of MppZL4 on *S.j* body were mainly located in syncytial cells.

Binding sites of MppZL4 on S.j body surface might be ALP or ALP-related proteins

To determine the activity of ALP in adult worms, infected mice were injected with ZL4 peptide, r12P, and PBS. The results showed that ALP activity in the body wall of worms was significantly decreased in ZL4 group. By contrast, a great amount of black precipitate was observed in the body wall of *S.j* worms treated with r12P or PBS, demonstrating the existence of abundant ALP (**Figure 6**, PBS results not shown). These data indicated that binding sites of MppZL4 on *S.j* body surface might be ALP or ALP-related proteins.

Discussion

In the first part of the study, we took the tails off *S.j* as research targets, used differential screening techniques and obtained MppZL4 peptide. The receptor of MppZL4 may be a type of protein related to surface membrane protein, which targets *S.j* [8, 9]. The study about the distribution and metabolism of MppZL4 showed that the number of the eluted phages in liver tissues was hundreds of times or even thousands of times of that in the lung tissues 2 h after MppZL4 injection. This is due to the fact that the liver is a reticuloendothelial system (RES) with a lot of scavenger receptors on the surface that can swallow and adsorb lots of phages [31, 32]. However, 6 h later, the number of phages in the lungs and liver tissues achieved the same order of magnitude, and the changes

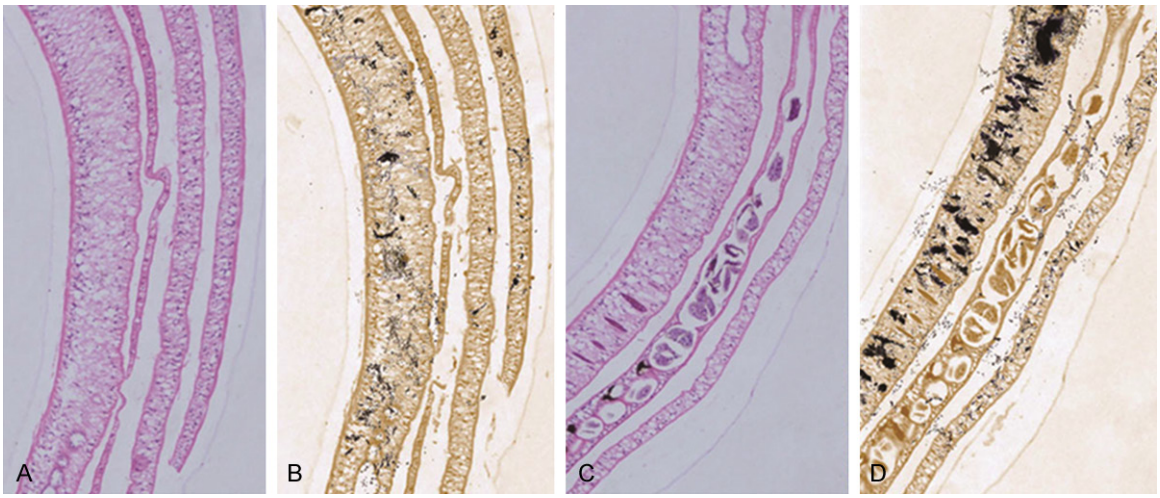

Figure 6. The effect of MppZL4 on alkaline phosphates activity in adult *Schistosoma japonicum*. A. Hematoxylin and eosin staining of *Schistosoma japonicum* from mice injected with MppZL4 (× 100). B. Gomori's staining of *Schistosoma japonicum* from mice injected with MppZL4 (× 100). C. Hematoxylin and eosin staining of *Schistosoma japonicum* from mice injected with random 12 peptides (× 100). D. Gomori's staining of *Schistosoma japonicum* from mice injected with random 12 peptides (× 100). Black precipitates observed in the body wall of *S.j* worms indicate alkaline phosphatase.

in phage abundance between the lungs and liver became comparable. Therefore, the key time points of subsequent experiments were arranged at 20 min, 6 h and 72 h after injection with phages.

Due to the particularity of the *S.j* epidermis and the complexity of the host body, the targeted peptides screened *in vitro* are not necessarily targeted *in vivo*. In normal mice, the abundance changes of MppZL4 in the liver and lungs tissues were not obvious. In addition, the abundance changes of M13KE in the liver and lungs tissues of infected mice were not obvious, either. However, the distributions of the phages were more even after 6 h. However, the abundance of MppZL4 showed obvious changes in infected mice. On day 3, the abundance was high in lung tissues and low in liver tissues; on day 10, it was on the contrary; on day 24, some of the mature worms migrated to the inferior mesenteric vein system, and the amount of worms in liver tissues was reduced, with MppZL4 abundance being reduced accordingly; on day 42, MppZL4 abundance in liver tissues was increased dramatically, which might be associated with the large number of eggs deposited in liver tissues.

DTI and DSI, the two main target indicators, were selected to evaluate the targeting effect of MppZL4 to *S.j* at different time points on different organs [17]. DTI was used to compare the tropism difference of different delivery systems, MppZL4 and M13KE, on the same organ (the liver or lungs of mice infected with *S.j*), while DSI was used to compare the tropism difference of the same delivery systems (MppZL4) on the same organ of different animal models (the liver or lungs of normal mice and mice infected with *S.j*). Values of DTI and DSI greater than 1.0 indicate that MppZL4 has targeting effect on target organs, with greater values corresponding to stronger targeting effects [17]. DTI and DSI values of eluted phages from the lungs on day 3, and those values of eluted phages from the liver on days 10, 24 and 42 were all much larger than 1.0. Of note, although DTI of MppZL4 from the liver of infected mice was 1.02 (greater than 1.0) on day 3, the eluted volume of MppZL4 in liver tissues was not significantly different from the negative control group or blank control group, and was much lower than that of MppZL4 in lung tissues. Therefore, the targeting effect of MppZL4 on the liver can be considered not significant at this time. Similarly, the targeting effect of MppZL4 on lung tissues was not significant on day 10, either.

The data presented in this study can fully demonstrate the targeting effect of MppZL4 at different time points. In the mice infected by *S.j*,

the abundance changes of MppZL4 in the liver and lungs were consistent with changes in the location of the worm's migration. However, MppZL4 had balanced distributions in the liver and lung tissues in normal mice. These results revealed that MppZL4 had targeted binding to *S.j* in mice. In addition, Western blotting confirmed the specific binding of MppZL4 to *S.j* worms at each phase in the mice.

MppZL4 is a molecule composed of ZL4 peptide and M13 phage. In order to test whether ZL4 peptide possesses targeting effect to *S.j*, we used Cy5.5 to label the N-terminal of ZL4 peptide (Cy5.5-ZL4) [25], and employed *in vivo* fluorescence imaging to study the targeting capability and biological distribution of Cy5.5-ZL4 in mice infected by *S.j*. Biological tissues have high light absorption in the visible range (350-600 nm) and the infrared range (> 900 nm). Near infrared refers to electromagnetic waves with wavelengths within 600-900 nm. Hemoglobin, water and lipid in living tissues rarely absorb light waves in near infrared region, so near infrared light can penetrate deeply into biological tissues, without too much effect on tissues. Near infrared fluorescence imaging technique can effectively avoid the interference from background fluorescence produced by organisms, and penetrate into tissues in a depth of 7-14 cm [33]. This technique significantly improves the efficiency of fluorescence detection and is particularly suitable for live imaging of small animals [34]. The *in vivo* half-life of near infrared cyanine dyes *in vivo* is short, with no specific selection on animal tissues. The covalent labeling of near infrared cyanine dyes has advantages of strong specificity, stable marking and long period of storage. Therefore, near infrared cyanine dyes are widely used for biological imaging in biomedical fields [35, 36]. Using near infrared optical imaging technique, we confirmed that MppZL4 targeted *S.j* in mice, and made preliminary analysis of the biological distribution and targeting capability of MppZL4. Of note, Cy5.5-MppZL4 showed strong optical signal in the kidneys of normal and infected mice, indicating that kidney is the primary metabolic pathway for Cy5.5-MppZL4 in mice [37].

Immunohistochemical experiments showed that MppZL4 mainly bound to the surface membrane of the *S.j* after 20 min, but was relocated to syncytial cells after 6 h, or even reached muscle cells [38, 39]. The fact that the positive rates of *S.j* worms at two time points were not significantly different, not only meant that the rate of phage-binding worms was independent of the metabolic rate of phages in mice, but also confirmed indirectly that the *S.j* wall had absorption function [40].

At 6 h time point, strong reactivity was evident on syncytial cells that contained rich ALP. Studies showed that ALP had different distribution in different developmental stages of *S.j* [41], strong positive reaction in miracidium period [11] and no enzymatic activity in the front part of the body in cercaria period [42]. When the worm matured, ALP levels in the tegument of the worms are rich. ALP is involved in the metabolism of nucleic acid and protein, playing an important role during the formation and maintenance of the skin [12-14]. MppZL4 is a type of phage that binds to the tail of *S.j* but not cercariae. KH_2PO_4 in the formula of PBS is an inhibitor of ALP [43], and the cercarial surface treated with PBS in difference panning process contains scarce ALP [8]. Western blotting analysis showed five specific binding bands using MppZL4 as the probe, among which the most significant band was about 24 kDa [8]. The molecular weight of *S.j* ALP protein SJCHGC07313 was 24.4 kDa [10]. Therefore, we hypothesized that MppZL4 binding sites on the tegument of *S.j* might be related to ALP or ALP-associated protein. Then, we tested the effect of MppZL4 on the activity of *S.j* ALP, and found that the activity of *S.j* ALP was decreased significantly after ZL4 exerted its effects.

In summary, this study demonstrated that MppZL4 had targeted binding effect on *S.j* with its binding site being associated with proteins related to *S.j* ALP. Although the targets and mechanisms of action have not been elucidated yet, the results have shown their significance. This study theoretically demonstrated that *S.j* tegument had a specifically binding site with exogenous peptides, offering new means to explore the interactions between hosts and parasites. In addition, MppZL4 can possibly be used as targeting molecules in worm-resistant drugs or as tracing molecules in imaging diagnosis technologies.

Acknowledgements

This work was supported by Hunan Provincial Young Foundation of China (No. 11B106), China

University Doctor Fund (No. 201036000Z110), and Hunan Provincial Natural Science Foundation of China (No. 11JJ3106).

Disclosure of conflict of interest

None.

Address correspondence to: Dr. Qingren Zeng, Centre of Cell and Molecular Biology Experiment, Xiangya School of Medicine, Central South University, 172 Tongzipo Road, Changsha 410013, Hunan Province, P.R. China. Tel: 86-734-8281390; Fax: 86-734-8281390; E-mail: zengqingren@126.com

References

[1] Huang SY, Deng ZH, Zhang QM, Lin RX, Zhang XC, Huo LC, Wang JL and Ruan CW. Endemic situation of schistosomiasis in Guangdong Province from 2004 to 2009. Zhongguo Xue Xi Chong Bing Fang Zhi Za Zhi 2011; 23: 197-8, 201.

[2] Zhu R, Qin ZQ, Feng T, Dang H, Zhang LJ and Xu J. XU Jing Assessment of effect and quality control for paracitological tests in national schistosomiasis surveillance sites. Zhongguo Xue Xi Chong Bing Fang Zhi Za Zhi 2013; 25: 11-5.

[3] Huang XY, Hang DR, Yang WZ, et al. Study on the accumulated temperature of Oncomelania snails and Schistosoma japonicum growth in areas related to the Eastern route of the South-to North Water Diversion Project. Journal of Pathogen Biology 2012; 7: 905-8.

[4] Wu CG, Xiao BZ, Li SS, et al. Surveillance report of schistosomiasis in potential prevalent areas in Chongqing city from 2008 to 2010. Journal of Tropical Medicine 2012; 12: 217-9.

[5] Dang H, Xu J, Li SZ, et al. Surveillance of schistosomiasis japonica in potential endemic areals in China. International Journal of Medical Parasitic Diseases 2011; 40: 71-6.

[6] An YW, Pang XL, Liu JB, et al. Surveillance of Schistosomiasis in the Mobile Population in Huadu, Guangdong. Journal of Tropical Medicine 2013; 13: 244-8.

[7] McManus DP, Gray DJ, Li Y, Feng Z, Williams GM, Stewart D, Rey-Ladino J and Ross AG. Schistosomiasis in the People's Republic of China: the Era of the Three Gorges Dam. Clin Microbiol 2010; 23: 442-66.

[8] Liu Y, Brindley PJ, Zeng Q, Li Y, Zhou J, Chen Y, Yang S, Zhang Z, Liu B, Cai L, McManus DP. Identification of phage display peptides with affinity for the tegument of Schistosoma japonicum schistosomula. Mol Biochem Parasitol 2011; 180: 86-98.

[9] Liu Y, Zhang ZP, Wang KG, Gu KZ, Cai LT and Zeng QR. Screening and Analysis of Peptides Specifically Binding to the Schistosomulum Tegument of Schistosoma japonicum. Zhongguo Ji Sheng Chong Xue Yu Ji Sheng Chong Bing Za Zhi 2013; 31: 27-32.

[10] Liu F, Lu J, Hu W, Wang SY, Cui SJ, Chi M, Yan Q, Wang XR, Song HD, Xu XN, Wang JJ, Zhang XL, Zhang X, Wang ZQ, Xue CL, Brindley PJ, McManus DP, Yang PY, Feng Z, Chen Z, Han ZG. New perspectives on host-parasite interplay by comparative transcriptomic and proteomic analyses of Schistosoma japonicum. PLoS Pathog 2006; 2: e29.

[11] Cesari IM, Ballen DE, Perrone T, Oriol O, Hoebeke J and Bout D. Enzyme Activities in Schistosoma mansoni Soluble Egg Antigen. J Parasitol 2000; 86: 1137-40.

[12] Gobert GN, McManus DP, Nawaratna S, Moertel L, Mulvenna J and Jones MK. Tissue Specific Profiling of Females of Schistosoma japonicum by Integrated Laser Microdissection Microscopy and Microarray Analysis. PLoS Negl Trop Dis 2009; 3: e469.

[13] Mulvenna J, Moertel L, Jones MK, Nawaratna S, Lovas EM, Gobert GN, Colgrave M, Jones A, Loukas A and McManus DP. Exposed proteins of the Schistosoma japonicum tegument. Int J Parasitol 2010; 40: 543-54.

[14] Bhardwaj R and Skelly PJ. Characterization of Schistosome Tegumental Alkaline Phosphatase (SmAP). PLoS Negl Trop Dis 2011; 5: e1011.

[15] Wang KG, Zeng QR, Yu ZY, Zeng TB and Liu Y. An Efficient and Accurate Method for Counting Target Molecules in Phage-Display Peptide Library. Zhongguo Ji Sheng Chong Xue Yu Ji Sheng Chong Bing Za Zhi 2011; 29: 236-8.

[16] Gipps EM, Arshady R, Kreuter J, Groscurth P and Speiser PP. Distribution of polyhexyl cyanoacrylate nanoparticles in nude mice bearing human osteosarcoma. J Pharm Sci 1986; 75: 256-8.

[17] Wang T, Baron K, Zhong W, Brundage R and Elmquist W. Bayesian Approach to Estimate AUC, Partition Coefficient and Drug Targeting Index for Studies with Serial Sacrifice Design. Pharm Res 2014; 31: 649-59.

[18] Stevens AJ, Martin SW, Brennan BS, Rowland M and Houston JB. Experimental determination of a drug targeting index for S(+) ibuprofen using the rat air pouch model of inflammation. J Drug Target 1994; 2: 333-9.

[19] Li J, Feng L, Fan L, Zha Y, Guo L, Zhang Q, Chen J, Pang Z, Wang Y, Jiang X, Yang VC, Wen L. Targeting the brain with PEG-PLGA nanoparticles modified with phage-displayed peptides. Biomaterials 2011; 32: 4943-50.

[20] Lehár J, Krueger AS, Avery W, Heilbut AM, Johansen LM, Price ER, Rickles RJ, Short GF 3rd, Staunton JE, Jin X, Lee MS, Zimmermann GR, Borisy AA. Synergistic drug combinations tend to improve therapeutically relevant selectivity. Nat Biotechnol 2009; 27: 659-66.

[21] John M. Walker. The Protein Protocols Handbook. 2nd edition. New Jersey: Humana Press Totowa; 2009. pp. 11-4.

[22] Wang D, Villasante A, Lewis SA and Cowan NJ. The mammalian beta-tubulin repertoire: hematopoietic expression of a novel, heterologous beta-tubulin isotype. J Cell Biol 1986; 103: 1903-10.

[23] Chen K, Yap LP, Park R, Hui X, Wu K, Fan D, Chen X and Conti PS. A Cy5.5-labeled phage-displayed peptide probe for near-infrared fluorescence imaging of tumor vasculature in living mice. Amino Acids 2012; 42: 1329-37.

[24] Massey S, Johnston K, Mott TM, Judy BM, Kvitko BH, Schweizer HP, Estes DM and Torres AG. In vivo bioluminescence imaging of Burkholderia mallei respiratory infection and treatment in the mouse model. Front Microbiol 2011; 2: 174.

[25] Li J, Zhang Q, Pang Z, Wang Y, Liu Q, Guo L and Jiang X. Identification of peptide sequences that target to the brain using in vivo phage display. Amino Acids 2012; 42: 2373-81.

[26] Wang KG, Zeng QR, Zhang YK, Zhou J, Cai LT, Liang Y and Liu Y. Preparation of Agar-Paraffin Double-Embedded Longitudinal Sections of Schistosoma japonicum. Zhongguo Ji Sheng Chong Xue Yu Ji Sheng Chong Bing Za Zhi 2012; 30: 415-7.

[27] Wei Q, Liu Y, Zeng QR, Chen YX, Zhou J, Liu BY, Zou Y, Yang SH, Cai LT, Li LX, Lan LM. Screening and Characterization of Peptides Specifically Binding to the Schistosomulum Tegument of Schistosoma japonicum. Zhongguo Ji Sheng Chong Xue Yu Ji Sheng Chong Bing Za Zhi 2010; 28: 172-5.

[28] Sameh Mohamed Farouk, Abdel-Hamid Kamel osman, Hussein Eidaroos Hussein and Said Mohamed Saleh Ammar. Prenatal histogenesis of uterine cervix of the one-humped camel (Camelus Dromedarius). Global Animal Science Journal 2013; 1: 1172-94.

[29] Huang YC, Zhu HM, Cai JQ, Huang YZ, Xu J, Zhou Y, Chen XH, Li XQ, Yang ZM, Deng L. Hypoxia inhibits the spontaneous calcification of bone marrow-derived mesenchymal stem cellS.j Cell Biochem 2012; 113: 1407-15.

[30] Caneguim BH, Beltrame FL, da Luz JS, Valentini SR, Cerri PS and Sasso-Cerri E. Primordial germ cells (spermatogonial stem cells) of bullfrogs express sex hormone-binding globulin and steroid receptors during seasonal spermatogenesis. Cells Tissues Organs 2013; 197: 136-44.

[31] Finger AN, Bisoff M, Wetterwald A, Gautschi E, Hohenfeld U, Klima I, Stadler BM, Mazzucchelli L, Thalmann GN, Cecchini MG. Scavenger receptor block as strategy for the identification of bone marrow homing phages by panning in vivo random peptide phage displayed librarieS.j Immunol Methods 2002; 264: 173-86.

[32] Smedsrød B, Pertoft H, Gustafson S and Laurent TC. Scavenger functions of the liver endothelial cell. Biochem J 1990; 266: 313-27.

[33] Zhang X, Bloch S, Akers W and Achilefu S. Near-infrared molecular probes for in vivo imaging. Curr Protoc Cytom 2012; Chapter 12: Unit12.27.

[34] Zhang HS, Wang H, Zhao YY. Molecular Probes and Detection Reagent. 1st edition. Beijing: Science Press; 2002.

[35] Funovics M, Weissleder R and Tung CH. Protease sensors for bioimaging. Anal Bioanal Chem 2003; 377: 956-63.

[36] Kobayashi H, Ogawa M, Alford R, Choyke PL and Urano Y. New strategies for fluorescent probe design in medical diagnostic imaging. Chem Rev 2010; 110: 2620-40.

[37] Deutscher SL. Phage display in molecular imaging and diagnosis of cancer. Chem Rev 2010; 110: 3196-211.

[38] Gobert GN, Stenzel DJ, McManus DP and Jones MK. The ultrastructural architecture of the adult Schistosoma japonicum tegument. Int J Parasitol 2003; 33: 1561-75.

[39] Ueberberg S and Schneider S. Phage library-screening: a powerful approach for generation of targeting-agents specific for normal pancreatic islet-cells and islet-cell carcinoma in vivo. Regul Pept 2010; 160: 1-8.

[40] Van Dorst B, De Coen W, Blust R and Robbens J. Phage display as a novel screening tool for primary toxicological targets. Environ Toxicol Chem 2010; 29: 250-5.

[41] Araujo-Montoya BO, Rofatto HK, Tararam CA, Farias LP, Oliveira KC, Verjovski-Almeida S, Wilson RA and Leite LC. Schistosoma mansoni: molecular characterization of Alkaline Phosphatase and expression patterns across life cycle stages. Exp Parasitol 2011; 129: 284-91.

[42] He YX and Yang HZ. Physiological studies on the post-cercarial development of Schistosoma japonicum. Acta Zoologica Sinica 1980; 26: 32-39.

[43] Hideaki Matsumoto and Tomoyuki Yamaya. Increase in Alkaline Phosphatase Activity in Cucumber Roots during Calcium Starvation. Plant Cell Physiol 1981; 22: 1137-40.